

for assessing the performance of all available current forecasts in the Balearic Sea and the southeastern Bay of Biscay. The models have shown varying levels of skills in predicting the trajectory of the observed drifters, depending on the region and on the analysed period, mainly related to their different capacities to reproduce coastal processes (e.g. inertial oscillations, submesoscale eddy activity, intensification of the Iberian poleward current) and diverse flow regimes (including seasonal modulation).

One surprising result is the better performance of some models when compared to the HF radar derived surface currents for some of the scenarios considered. As the skill score is region-dependant and scenario-specific, this might not be a general rule, and more similar experiments are needed to be able to draw some conclusions. Furthermore, it should be considered that skill scores computed at the model domain boundaries and in areas with higher HF radar observational errors penalises the overall results.

Findings highlight the need of including this type of skill assessment services to evaluate and monitor the performance of operational systems and the accuracy of its products in order to unlock their potential for different applications.

Acknowledgements

The development of the presented downstream service is supported by Mercator Ocean International throughout the CMEMS-User Uptake IBISAR project (CMEMS User Uptake, contract ref. 67-UU-DO-CMEMS-DEM4_LOT7). Authors wish to thank Copernicus Marine Service for making model and in-situ data products available, the Spanish Port System (PUERTOS) for the datasets of SAMOA, SASEMAR for providing the data of the drifter buoys of the Bay of Biscay and their feedback on the service, EUSKOOS and the Directorate of Emergency Attention and Meteorology of the Basque Government for the HF radar surface current datasets of the Bay of Biscay and SOCIB for HF radar data in the Ibiza Channel and the WMOP forecasts. The Lagrangian models developed in the context of the COSMO project (ref. CTM2016-79474-R, MINECO/FEDER, UE) are used in this study. IBISAR service is generated using E.U. Copernicus Marine Service Information.

Section 3.5: Surface picture of the Levantine Basin as derived by drifter and satellite data

Authors: Milena Menna, Giulio Notarstefano, Pierre-Marie Poulain, Elena Mauri, Pierpaolo Falco, Enrico Zambianchi

Statement of main outcome: Ocean circulation derived from drifter data covers not only oceanographic and climate research but also spread and retention of pollutants. The latter field has a strong societal impact because it is able to give the measure of political action efficiency in such a delicate sector. Moreover, it is able to actively improve the policy-making of the environmental governance. The scientific knowledge derived from such a topic is transferable easily to the public in an accessible form to benefit the relationship between science and society and to respond better to the human needs.

The surface circulation in the Levantine Basin derives from the complex interaction among multi-scale flow patterns, producing a high spatio-temporal variability of the current field. A considerable amount of in situ data has been collected in this region, giving us the opportunity to produce an updated version of the surface current paths (1993–2018). Drifter data are compared with satellite altimetry data in order to define a detailed and complete picture of the main quasi-permanent structures and of the along-slope currents. This updated description of the circulation pattern reinforces the work of the scientific-societal communities in defining the southeastern Levantine basin as the most critical area of marine litter accumulation.

Data use:

Ref. No.	Product name and type	Documentation
3.5.1	SEALEVEL_MED_PHY_L4_NRT_OBSERVATIONS_008_050 SEALEVEL_MED_PHY_L4_REP_OBSERVATIONS_008_051	PUM: http://marine.copernicus.eu/documents/PUM/CMEMS-SL-PUM-008-032-051.pdf QUID: http://marine.copernicus.eu/documents/QUID/CMEMS-SL-QUID-008-032-051.pdf
3.5.2	INSITU_MED_NRT_OBSERVATIONS_013_035	PUM: http://marine.copernicus.eu/documents/PUM/CMEMS-INS-PUM-013.pdf QUID: http://marine.copernicus.eu/documents/QUID/CMEMS-INS-QUID-013-030-036.pdf

3.5.1. Introduction

The marine litter has really become a serious problem in the Mediterranean Sea. This issue is intensified by the limited exchanges of the Mediterranean with the open ocean, the high degree of urbanisation along the coasts and the high level of maritime traffic. The pollution caused by marine litter can deeply impact human and animal health and create an economic damage to the societal environment. The most abundant marine litter items worldwide are plastics (Gregory and Ryan 1997)

and they constitute more than 80% of the floating debris in the Mediterranean Sea (Galgani 2014; Suaria and Aliani 2014). Their persistence in the marine environment and their slow degree of degradation (Barnes et al. 2009) make the plastics a threat that has to be monitored and possibly reduced.

The geography of the Mediterranean basin and its general surface circulation scheme contribute to create a sort of re-circulation system of floating debris in which they are distributed into possibly retention and stranding areas within the basin.

Recently, Lagrangian models and in-situ data have been used to estimate the drift of floating debris (Mansui et al. 2015; Liubartseva et al. 2018) and the probability of debris particles to reach different areas of the Mediterranean basin (Zambianchi et al. 2017). The results of the mentioned studies have defined the Southern Levantine basin as a sort of ‘garbage patch’ of the Mediterranean, where the surface currents contribute to enhance the local increase of floating litter (Zambianchi et al. 2017). In particular, the southern coast of the Levantine seems to be a site of destination/accumulation of pollution that extent also towards Syria and the Cilician area (Mansui et al. 2015; Liubartseva et al. 2018). Currently, the statistics performed in Zambianchi et al. (2017) are based on Lagrangian drifter data updated to 2014. The aim of this work is to provide an updated version of the surface circulation patterns in the Levantine sub-basin, adding the copious drifter data collected after 2014.

3.5.2. Results and discussion

Drifter velocities (CMEMS product Ref. No. 3.5.2), collected in the Levantine basin during the period 1993–2018 (Figure 3.5.1), are compared with the concurrent satellite altimetry products (Absolute Dynamic Topography – ADT, CMEMS product Ref. No. 3.5.1) in order to add new and further insights to the mean and seasonal circulation patterns of this area. More details about the drifter data processing are available in Menna et al. (2017, 2018).

The two datasets fit rather well (Figure 3.5.1(b)) and define the well-known cyclonic coastal circuit in the Levantine sub-basin (Menna et al. 2012) with strength as large as 15 cm/s along the southern and eastern coasts (Libyo-Egyptian Current – LEC) and larger than 25 cm/s along the northern coast (Cilician Current – CC – and Asia Minor Current – AMC), in agreement with the results of Menna et al. (2012). The interior of the Levantine basin is longitudinally divided into two parts by the zonal meandering Mid-Mediterranean Jet (MMJ; speeds of 10–15 cm/s), with prevalent anticyclonic/cyclonic

structures located southern/northern of the MMJ pathway. For some years after the publication of Millot and Taupier-Letage (2005) and Millot and Gerin (2010) there was a debate about the existence of the MMJ. According to the above-mentioned authors, the MMJ may not be a proper eastward current but it can correspond to the northern limb of the anticyclonic eddies generated by the instability of the along-slope LEC. Nevertheless, the work published thereafter by Menna et al. (2012), Poulain et al. (2012), Schroeder et al. (2012) and more recently by Mauri et al. (2019) demonstrate unambiguously the existence of the MMJ.

The main anticyclonic structures that characterise the surface current field south of the MMJ signature are the mesoscale Egyptian eddies (EE; speeds of 10 cm/s) derived from the instability of the along-slope current (Hamad et al. 2005, 2006; Menna et al. 2012), the sub-basin scale Mersa-Matruh Gyre (MMG; maximum speeds of ~ 25 cm/s) and Cyprus Gyre (CG, mean speeds of 10–20 cm/s) (Gertman et al. 2007; Mauri et al. 2019). The Shikmona Eddy (ShE) is defined in literature as a very complex system, composed of several cyclonic and anticyclonic eddies (Gertman et al. 2007; Mauri et al. 2019), and formed as pinched off meanders from the instability of the coastal current (Menna et al. 2012); its position, sizes and intensities vary markedly over time (Mauri et al. 2019). The mean pattern of the ShE is cyclonic (Figure 3.5.1(b)) in the period 1993–2018.

The main cyclonic structures located north of the MMJ signature (Figure 3.5.1(b)) are the sub-basin scale Western Cretan Gyre (WCG; speeds of 10–15 cm/s) and the Rhodes Gyre (RG; speeds of 15–25 cm/s). In addition to these large cyclones, there is a mesoscale cyclonic eddy generally squeezed between Syria and the eastern Cyprus coasts, known as Latakia Eddy (LTE; speeds of 10 cm/s). The LTE is generated by the interaction between the MMJ and the northward coastal current (Zodiatis et al. 2003; Menna et al. 2012). The cyclonic pattern along the northern coasts of the Levantine is interrupted only by the anticyclonic, wind-driven Ierapetra Gyre (IG; speeds of 15 cm/s), induced by the northeasterly Etesian winds (Amitai et al. 2010). Altimetry data point out another cyclonic mesoscale structure (centred at 33.7°N and 25.3°E) that has never been described before in literature as a stand-alone structure, but sometimes it is included in the WCG system (e.g. Poulain et al. 2012; Pinardi et al. 2015). The occurrence of a recurrent cyclonic structure in this region is confirmed by the DYNED-Atlas database (Le Vu et al. 2017; <https://dyned.cls.fr/seewater/#!&page=isv-mainPage>), that uses the Angular Momentum Eddy Detection Algorithm in the period 2000–2017, to locate and track the surface signature of mesoscale eddies in

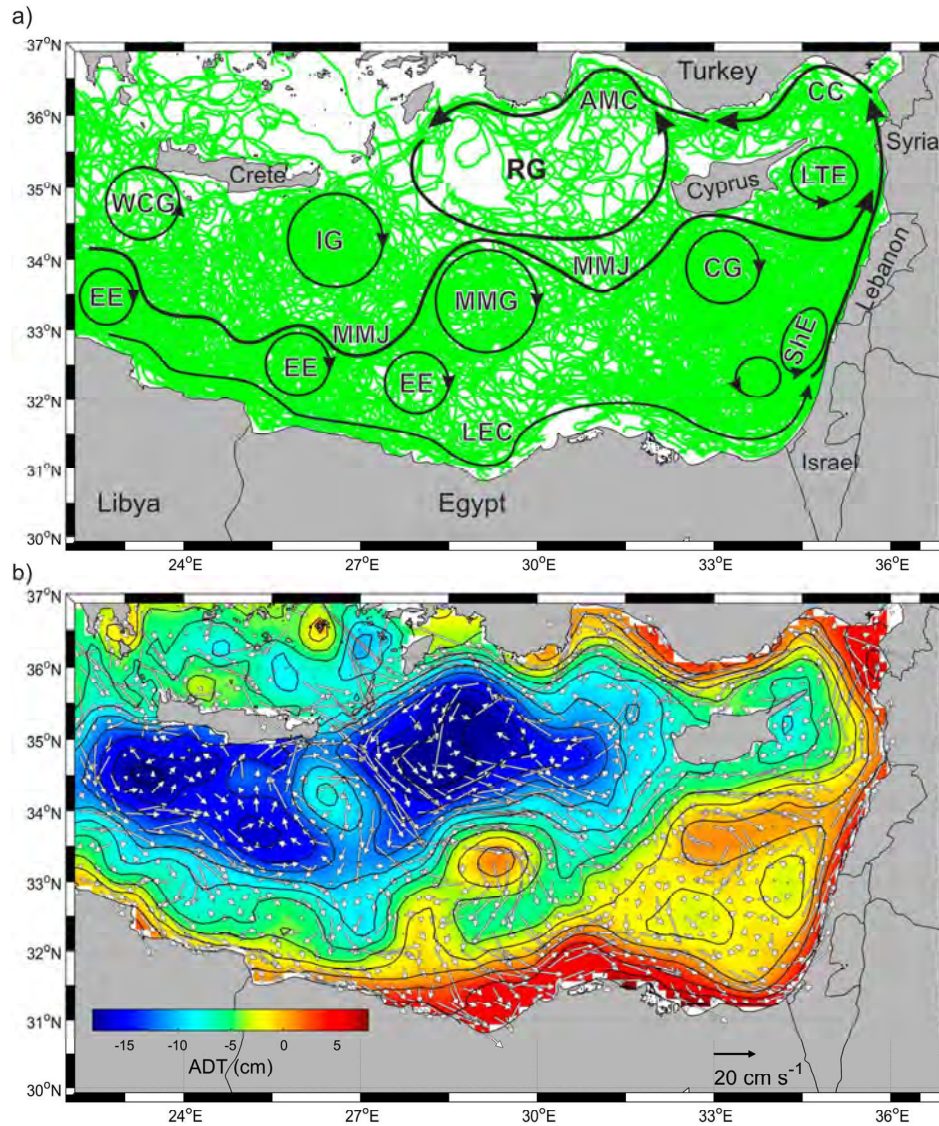


Figure 3.5.1. (a) Drifter trajectories and (b) mean drifter currents (arrows, CMEMS product Ref. No. 3.5.2) in bins of $0.25^\circ \times 0.25^\circ$ superimposed on the mean map of ADT (CMEMS product Ref. No. 3.5.1) between 1993 and 2018. Black arrows in (a) emphasise the location of the main currents, sub-basin and mesoscale eddies and gyres adapted from Menna et al. (2012); acronyms are defined in the text. Black contour lines in (b) are referred to the ADT field.

the Mediterranean Sea. The DYNED-Atlas database describes a cyclonic structure whose core is located between 33.4°N and 34.3°N and between 24.7°E and 25.7°E for over a third of the 17 years analysed. This mesoscale cyclone, located southwest of the IG, is defined hereafter as Southern Cretan Eddy (SCE; speeds of 5–10 cm/s). Drifter derived currents do not clearly identify the edge of the SCE (due to their non-homogenous spatial and temporal sampling) but detect the occurrence of a cyclonic meander in this region.

The seasonal variability of the surface currents field was estimated dividing the dataset in two extended seasons, selected following the suggestion of Menna et al. (2012): the extended winter corresponds to January–

June (Figure 3.5.2(a)), and the extended summer to July–December (Figure 3.5.2(b)). The dataset used in this work allows to add more details than the previous literature on the seasonal variability of circulation structures, especially in the easternmost part of the Levantine where, after 2010, a conspicuous amount of drifter data was collected in the framework of some international projects. The WCG, IG, MMG, and the southern limb of the RG are more dynamic in summer (Figure 3.5.2(b); speeds up to 30 cm/s), as well as the CC, AMC and the LTE (speeds larger than 20 cm/s). The CG is more intense in winter (Figure 3.5.2(b); speeds of 10–15 cm/s), whereas it appears weaker and zonally elongated during summer (Figure 3.5.2(b); speeds of

10–15 cm/s). The ADT values are generally higher in summer. The SCE is a permanent structure observed in both the seasons with greater intensity during summer (speeds of 18 cm/s); its shape and location are influenced by the seasonal and interannual variability of IG.

The year 2018 is characterised by higher intensity of the anticyclonic structures (Figure 3.5.3(a)) compared to the mean field of the period 1993–2018 (Figure 3.5.1 (b)). Drifters entrapped in the MMG show a strengthening of this feature (speeds larger than 40 cm/s) and an

increase of its longitudinal extension (diameter of about 400 km). The centre of the CG (Figure 3.5.3(a)) is shifted to the west with respect to its mean location (Figure 3.5.1(b)), and the main lobe of the ShE is anticyclonic and located south east of Cyprus (Figure 3.5.3 (a)). The cyclonic activity is weakened in the region of the RG and the SCE disappears (Figure 3.5.3(a)). The sea level rises almost everywhere with larger increments along the coasts, in the IG and MMG and south of Cyprus (Figure 3.5.3(b)).

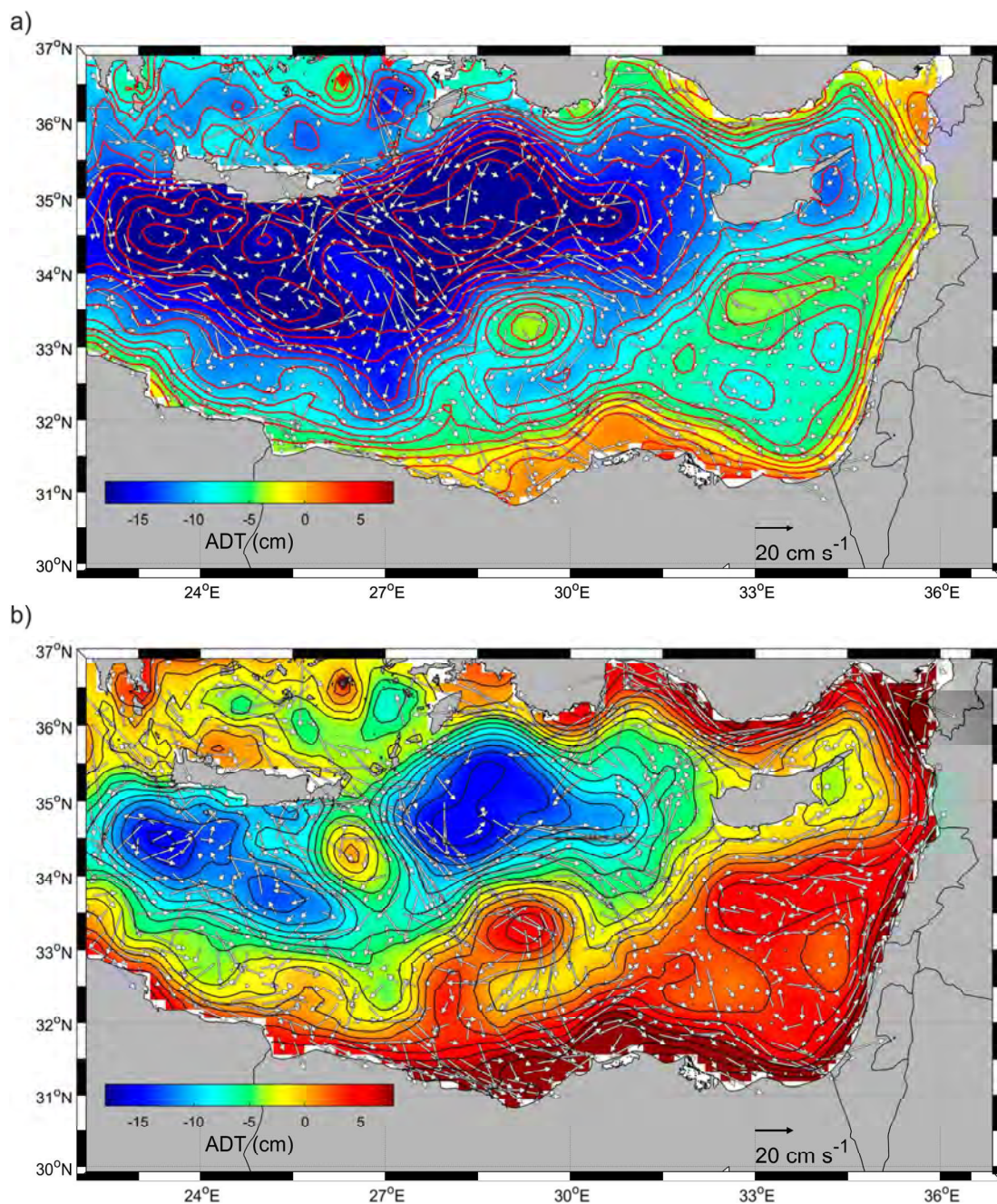


Figure 3.5.2. Mean drifter currents (arrows, CMEMS product Ref. No. 3.5.2) in bins of 0.25°x 0.25° superimposed on mean map of ADT (CMEMS product ref. No. 3.5.1) in the extended winter (a) and extended summer (b). Contour lines refer to the ADT field.

Model results by [Zambianchi et al. \(2017\)](#) represent probabilities of finding particle retention areas based on the transition matrix of drifters deployed in the Mediterranean and floating until 2014, showing a marked asymptotic maximum in the southeastern Levantine basin. The above discussed more recent drifter data show, in particular, an intensification of anticyclonic eddies developing in that same area, namely south of the MMJ. As recently

discussed by [Brach et al. \(2018\)](#) in a comparative analysis between cyclonic and anticyclonic eddies in a similar context, the latter show a much stronger capacity to entrap litter particles. For this reason, we expect that the situation of 2018 may have led to an even enhanced accumulation off the coasts of Libya and Egypt, and a possible resulting northeastward migration as hypothesised by [Liubartseva et al. \(2018\)](#).

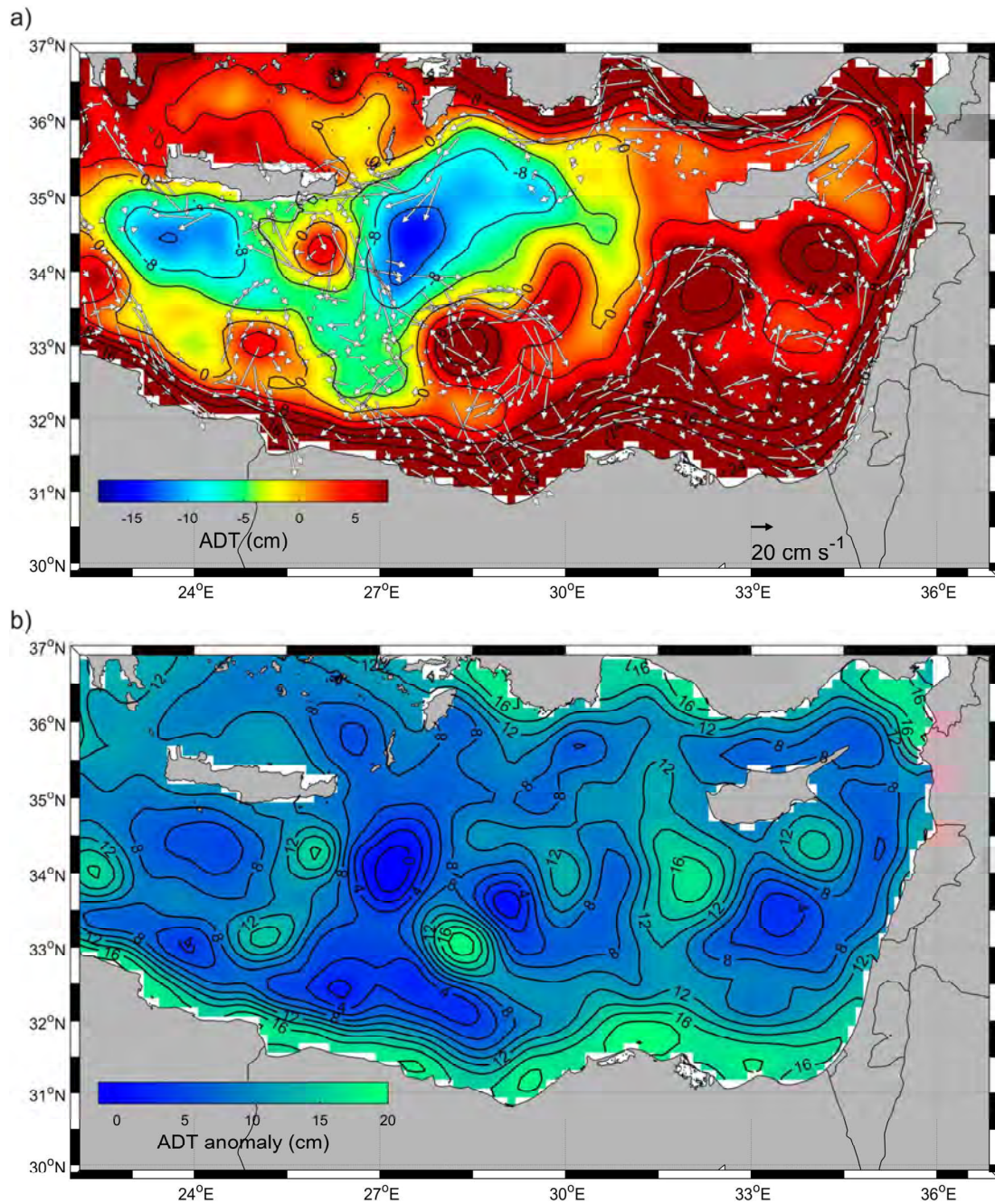


Figure 3.5.3. Mean drifter currents (arrows, CMEMS product Ref. No. 3.5.2) in bins of 0.25°x0.25° superimposed on the mean map of ADT (colours, CMEMS product Ref. No. 3.5.1) in 2018 (a); anomaly of the ADT field in 2018 with respect to the period 1993–2018 (b).

3.5.3. Conclusions

The Mediterranean drifter dataset updated to 2018 not only provides more data but also guarantees a more complete spatial and temporal coverage in areas that were previously less sampled (like the northern part of the Levantine sub-basin).

The improvement of the drifter dataset is fundamental in strengthening and supporting present and future studies on the transport of marine litter. Indeed, a more detailed and robust description of the main currents and sub-basin/mesoscale structures (eddies and gyres) has been provided in this work: the SCE has been mentioned here for the first time and the CC and AMC are now much better tracked in winter seasons. It has been recently declared that the Mediterranean is most likely one of the areas of the global ocean most strongly impacted by the presence of microplastics (see, e.g. Suaria et al. 2016); within the Mare Nostrum, the Levantine sub-basin is a highly marine litter contaminated area and a deeper knowledge of the floating matter propagation is necessary to deeply understand the mechanisms of the waste dispersion. The drifter dataset will help in this context, providing a more robust description of the current field that will favour the learning mechanism of the distribution, retention and accumulation of the marine floating debris in the Mediterranean Sea and in particular in the Levantine sub-basin. This implies that enhancing the Lagrangian dataset is of great importance not only for the advancement of the knowledge of the mechanisms governing the dynamical functioning of the Mediterranean, but also for the strong societal impact that a deeper awareness of local dispersion processes may provide to the assessment of marine litter distribution and to the design of possible mitigation strategies of such a critical environmental issue.

Note

1. <https://data.worldbank.org/indicator/ny.gdp.defl.zs>.

References

Section 3.1: Evidence of the TOPEX – A Altimeter Instrumental Anomaly and Acceleration of the Global Mean Sea Level.

- Ablain M, Meyssignac B, Zawadzki L, Jugier R, Ribes A, Cazenave A, Picot N. 2018. Error variance-covariance matrix of global mean sea level estimated from satellite altimetry (TOPEX, Jason 1, Jason 2, Jason 3). *Seanoë*. DOI:10.17882/58344.
- Ablain M, Jugier R, Zawadzki L, Taburet N, Cazenave A, Meyssignac B, Picot N. 2017. The TOPEX-A drift and impacts on GMSL time series. Poster presentation, OSTST 2017. [accessed 2019 April 11]. https://meetings.aviso.altimetry.fr/fileadmin/user_upload/tx_ausycslsseminar/files/Poster_OSTST17_GMSL_Drift_TOPEX-A.pdf.
- Ablain M, Legeais JF, Prandi P, Fenoglio-Marc L, Marcos M, Benveniste J, Cazenave A. 2017. Satellite altimetry-based sea level at global and regional scales. *Surv Geophys* 38:9–33. DOI:10.1007/s10712-016-9389-8.
- Ablain M, Meyssignac B, Zawadzki L, Jugier R, Ribes A, Cazenave A, Picot N. 2019. Uncertainty in satellite estimate of global mean sea level changes, trend and acceleration, *Earth Syst Sci Data*. 11:1189–1202. DOI:10.5194/essd-11-1189-2019.
- Ablain M, Philipps S. 2005. AVISO 2005 annual report on TOPEX/Poseidon validation activities. CLS.DOS/NT/05.240. SALP-RP-MA-EA-21315-CLS. [accessed 2019 May 24]. https://www.aviso.altimetry.fr/fileadmin/documents/calval/validation_report/TP/annual_report_tp_2005.pdf.
- Beckley BD, Callahan PS, Hancock DW, Mitchum GT, Ray RD. 2017. On the ‘Cal-mode’ correction to TOPEX satellite altimetry and its effect on the global mean sea level time series. *J Geophys Res C Oceans*. 122(11):8371–8384. DOI:10.1002/2017jc013090.
- Birkmann J, Licker R, Oppenheimer M, Campos M, Warren R, Luber G, O’Neill BC, Takahashi K. 2014. Cross-chapter box on a selection of the hazards, key vulnerabilities, key risks, and emergent risks identified in the WGII contribution to the fifth assessment report. In: Field CB, Barros VR, Dokken DJ, Mach KJ, Mastrandrea MD, Bilir TE, Chatterjee M, Ebi KL, Estrada YO, Genova RC, Girma B, Kissel ES, Levy AN, MacCracken S, Mastrandrea PR, White LL, editors. *Climate change 2014: impacts, adaptation, and vulnerability. Part A: global and sectoral aspects. Contribution of working group ii to the fifth assessment report of the intergovernmental panel on climate change*. Cambridge: Cambridge University Press; p. 113–121.
- Cazenave A, Le Cozannet G. 2014. Sea level rise and coastal impacts. *Earth’s Fut*. 2(2):15–34.
- Cazenave A, Palanisamy H, Ablain M. 2018. Contemporary sea level changes from satellite altimetry: what have we learned? What are the new challenges? *Adv Space Res*. 62(7):1639–1653. DOI:10.1016/j.asr.2018.07.017.
- Chen X, Zhang X, Church JA, Watson CS, King MA, Monselesan D, Legresy B, Harig C. 2017. The increasing rate of the global mean sea level rise during 1993–2014. *Nat Clim Change*. DOI:10.1038/nclimate3325.
- Cheng LK, Trenberth E, Fasullo J, Boyer T, Abraham J, Zhu J. 2017. Improved estimates of ocean heat content from 1960 to 2015. *Sci Adv*. 3:3. DOI:10.1126/sciadv.1601545.
- Church J, White N, Arblaster J. 2005. Significant decadal-scale impact of volcanic eruptions on sea level and ocean heat content. *Nature*. 438:74–77. DOI:10.1038/nature04237.
- Church JA, Clark PU, Cazenave A, Gregory JM, Jevrejeva S, Levermann A, Merrifield MA, Milne GA, Nerem RS, Nunn PD, et al. 2013. Sea level change. In: Stocker TF, Qin D, Plattner G-K, Tignor M, Allen SK, Boschung J, Nauels A, Xia Y, Bex V, Midgley PM, editors. *Climate change 2013: the physical science basis. contribution of working group I to the fifth assessment report of the intergovernmental panel on climate change*. Cambridge: Cambridge University Press.
- Church JA, White NJ. 2011. Sea-level rise from the late 19th to the early 21st century. *Surv Geophys*. 32:585. DOI:10.1007/s10712-011-9119-1.

- Copernicus European State of the Climate: Sea Level. 2019. <https://climate.copernicus.eu/sea-level>. https://climate.copernicus.eu/sites/default/files/2019-04/Brochure_Final_Interactive_1.pdf, last access: 23/05/2019.
- Couhert A, Cerri L, Legeais JF, Ablain M, Zelensky N, Haines B, Lemoine F, Bertiger W, Desai S, Otten M. 2014. Towards the 1 mm/y stability of the radial orbit error at regional scales. *Adv Space Res.* DOI:10.1016/j.asr.2014.06.041.
- Dangendorf S, Marcos M, Wöppelmann G, Conrad CP, Frederikse T, Riva R. 2017. Reassessment of 20th century global mean sea level rise. *Proc Natl Acad Sci.* 114 (23):5946–5951. DOI:10.1073/pnas.1616007114.
- Dasgupta S, Laplante B, Meisner C, Wheeler D, Yan J. 2009. The impact of sea level rise on developing countries: a comparative analysis. *Clim Change.* 93(3–4):379–388.
- Decharme B, Delire C, Minvielle M, Colin J, Vergnes J-P, Alias A, Saint-Martin D, Sférian R, Sénési S, Voltaire A. 2019. Recent changes in the ISBA-CTRIP land surface system for Use in the CNRM-CM6 climate model and in global Off-line Hydrological applications. *J Adv Model Earth Syst.* 11(5):1207–1252. DOI:10.1029/2018MS001545.
- Dieng HB, Cazenave A, Meyssignac B, Ablain M. 2017. New estimate of the current rate of sea level rise from a sea level budget approach. *Geophys Res Lett.* 44:3744–3751.
- Escudier P, Couhert A, Mercier F, Mallet A, Thibaut P, Tran N, Amarouche L, Picard B, Carrère L, Dibarboue G, et al. 2017. Satellite radar altimetry: principle, geophysical correction and orbit, accuracy and precision. In: Stammer D, Cazenave A, editors. *Satellite altimetry over oceans and land surfaces*. Boca Raton (FL): CRC Press, Taylor & Francis; p. 1–70.
- Fasullo J, Nerem R, Hamlington B. 2016. Is the detection of accelerated sea level rise imminent? *Sci Rep.* 6:31245. DOI:10.1038/srep31245.
- Gleckler PJ, AchutaRao K, Gregory JM, Santer BD, Taylor KE, Wigley TML. 2006. Krakatoa lives: the effect of volcanic eruptions on ocean heat content and thermal expansion. *Geophys Res Lett.* 33:17. DOI:10.1029/2006GL026771.
- Gouretski V, Reseghetti F. 2010. On depth and temperature biases in bathythermograph data: development of a new correction scheme based on analysis of a global ocean database. *Deep Sea Research I.* 57(6):812–833. DOI:10.1016/j.dsr.2010.03.011.
- Gregory JM, Lowe JA, Tett SFB. 2006. Simulated global-mean sea level changes over the last half-millennium. *J Clim.* DOI:10.1175/JCLI3881.1.
- Hay CC, Morrow E, Kopp RE, Mitrovica JX. 2015. Probabilistic reanalysis of twentieth-century sea-level rise. *Nature.* 517:481–484. DOI:10.1038/nature14093.
- Hayne GS, Hancock DW. 1998. Observations from long-term performance monitoring of the TOPEX radar altimeter. TOPEX/Poseidon/Jason-1 Science Working Team Meeting, Keystone.
- Hinkel J, Lincke D, Vafeidis AT, Perrette M, Nicholls RJ, Tol RSJ, Marzeion B, Fettweis X, Ionescu C, Levermann A. 2014. Future coastal flood damage and adaptation costs. *Proc Natl Acad Sci USA.* 111(9):3292–3297. DOI:10.1073/pnas.1222469111.
- Jevrejeva S, Jackson LP, Grinsted A, Lincke D, Marzeion B. 2018. Flood damage costs under the sea level rise with warming of 1.5 °C and 2 °C. *Environ Res Lett.* 13 (7):074014. <https://iopscience.iop.org/journal/1748-9326>.
- Jevrejeva S, Moore JC, Grinsted A, Matthews AP, Spada G. 2014. Trends and acceleration in global and regional sea levels since 1807. *Global Planet Change.* 113:11–22. DOI:10.1016/j.gloplacha.2013.12.004.
- Jouzel J. 2015. Rapport « Le climat de la France au XXIe siècle », ministère de l'Écologie, du Développement durable et de l'Énergie. Volume 5 mars 2015 p.40. <http://www.senat.fr/rap/r15-014/r15-0143.html>.
- Kebede AS, Nicholls RJ. 2012. Exposure and vulnerability to climate extremes: population and asset exposure to coastal flooding in Dar es Salaam, Tanzania. *Reg Environ Change.* 12:81–94.
- Kleinherenbrink M, Riva R, Scharroo R. 2019. A revised acceleration rate from the altimetry-derived global mean sea level record. *Sci Rep.* 9:10908. DOI:10.1038/s41598-019-47340-z.
- Legeais J-F, Ablain M, Thao S. 2014. Evaluation of wet troposphere path delays from atmospheric reanalyses and radiometers and their impact on the altimeter sea level. *Ocean Sci.* 10:893–905. DOI:10.5194/os-10-893-2014.
- Legeais J-F, Ablain M, Zawadzki L, Zuo H, Johannessen JA, Scharffenberg MG, Fenoglio-Marc L, Fernandes MJ, Andersen O, Rudenko S, Cipollini P. 2018. An accurate and homogeneous altimeter sea level record from the ESA climate change initiative. *Earth Syst Sci Data Discuss.* 1–35. DOI:10.5194/essd-2017-116.
- Legeais J-F, von Schuckmann K, Melet A, Storto A, Meyssignac B. 2018. Sea level, in Copernicus marine service ocean state report, issue 2. *J Oper Oceanogr.* 11(S1):s13–s16. DOI:10.1080/1755876X.2018.1489208.
- Levitus S, Antonov JI, Boyer TP, Baranova OK, Garcia HE, Locarnini RA, Mishonov AV, Reagan JR, Seidov D, Yarosh ES, Zweng MM. 2012. World ocean heat content and thermocline sea level change (0–2000 m), 1955–2010. *Geophys Res Lett.* 39:L10603. DOI:10.1029/2012GL051106.
- Llovel W, Guinehut S, Cazenave A. 2010. Regional and inter-annual variability in sea level over 2002–2009 based on satellite altimetry, Argo float data and GRACE ocean mass. *Ocean Dyn.* 60:1193–1204. DOI:10.1007/s10236-010-0324-0.
- Llovel W, Willis JK, Landerer FW, Fukumori I. 2014. Deep-ocean contribution to sea level and energy budget not detectable over the past decade. *Nat Clim Change.* 4:1031–1035.
- Marzeion B, Jarosch AH, Hofer M. 2012. Past and future sea-level change from the surface mass balance of glaciers. *Cryosphere.* 6:1295–1322. DOI: 10.5194/tc-6-1295-2012.
- McGranahan G, Balk D, Anderson B. 2007. The rising tide: assessing the risks of climate change and human settlements in low elevation coastal zones. *Environ Urban.* 19(1):17–37. DOI:10.1177/0956247807076960.
- Nerem RS, Beckley BD, Fasullo J, Hamlington BD, Masters D, Mitchum GT. 2018. Climate change driven accelerated sea level rise detected in the altimeter era. *PNAS.* 115 (9):2022–2025.
- Nerem S, Ablain M, Cazenave A. 2017. A 25-year long satellite altimetry-based global mean sea level record; closure of the sea level budget & missing components. In: Stammer C, editor. *Satellite altimetry over oceans and land surfaces*. Boca Raton (FL): CRC Press, Taylor & Francis; p. 187–210.